European Geosciences Union General Assembly 2017, EGU
Division Energy, Resources & Environment, ERE

Numerical investigations of upward migration of fracking fluid along a fault zone during and after stimulation

Reza Taherdangkoo*, Alexandru Tatomir, Robert Taylor, Martin Sauter

Department of Applied Geology, Geosciences Center, University of Göttingen, Goldschmidtstr. 3, D-37077 Göttingen, Germany

Abstract

This study investigates the potential contamination as a result of hydraulic fracturing operations in the vicinity of a conductive fault zone. The general aim is to determine and rank key parameters with the most important influence on upward transport of fracking fluid from a hydrocarbon bearing formation (source) towards a shallow groundwater aquifer (receptor) via a conductive fault (pathway). Simulation results show that the fault zone properties and hydraulic fracturing pressure strongly dominate fluid transport towards the aquifer horizon. Nevertheless, the probability of contamination of shallow groundwater from fracturing fluid migration is low.

Keywords: hydraulic fracturing; fracturing fluid; numerical modelling; fault zone; shale gas reservoir;

1. Introduction

During the last decade, hydrocarbon production using unconventional resources (e.g., "shale gas" and "tight gas"-TG reservoirs) gained considerable attention from the oil and gas industry to cover the global increase in energy demand. In contrast to conventional gas reservoirs, shale reservoirs display relatively low matrix permeabilities, thus making it difficult and energy inefficient to produce the gas using standard procedures. Hydraulic fracturing (HF) improves access to the larger part of the reservoir by creating artificial fracture networks increasing reservoir permeability and the contact areas across which fluids flow from the matrix to the fractures [1]. The generally applied method of HF involves a stage-based, high-pressurized "fracking fluid (FF)" injection into the hydrocarbon bearing

* Corresponding author. Tel.: +49-551-399267; fax: +49-551-399379
E-mail address: reza.taherdangkoo@geo.uni-goettingen.de

formation (HCBF), for a short period of time [2–7]. Following the artificial fracture system formation, reservoir pressure is dissipated because of "flowback", a process which mobilized methane and reservoir fluids displace FF being pumped back to the surface [6,8].

Recently, the EU funded "FracRisk" project within the Horizon 2020 framework program has initiated efforts to investigate the probability of in-situ contamination possibilities of hydraulic fracturing operation in HCBF. The plan devised to further the field's knowledge base is to apply a features (i.e. site/region physical characteristics), events (i.e. earthquakes), and processes (i.e. diffusion, advection) - FEP - generic modeling approach. An FEP database was constructed and provided in a discussion platform to identify, rank, and assess the most critical failure scenarios in HF operations (D31, D32, D41) [4,5,7]. This research method dissects the topic by individually researching six possible contamination scenarios in detail, in which the identification and connections of sources (i.e. TG reservoirs), pathways (e.g., faults), and targets/receptors (e.g., neighboring aquifers) are evaluated [5,6].

Currently, there is only a limited volume of numerical modeling based research analyses that explore this particular pathway are actually available[2,8–12]. Majority of them employ a rather similar conceptual approach, which include a deep HCBF, an overburden, and an aquifer, to investigate vertical HF fluid migration through a permeable pathway extending from the HCBF to an above-lying aquifer. However, they vary with respect to assigned boundary and initial conditions, physical rock and fluid properties, flow-driving mechanisms, and depths of geologic strata. Myer [8] produced a Marcellus shale-based model to support claims of pressure induced FF transport from shale to aquifer. Based on Myer investigation, HF can potentially promote fluid fluxes from a shale formation and reduce the travel time to an overlying aquifer. He concluded the presence of a permeable pathway decreasing travel time for an upward transport of fluids. Kissinger et al. [2] presented three different scenarios addressing the short- and long-term movement of FFs, brine and methane into an overburden applying both local and regional scales. Gassiat et al. [10] utilized a simplified, two-dimensional conceptual model with parameter values sourced from a combination of shale gas formations to assess the long-term (5000 years) impact of FF migration into geological layers resulting from HF operations within an overpressurized shale reservoir. Birdsell et al. [12] presented a two-dimensional conceptual model that accounted for injection, production, capillary imbibition, and buoyancy forces. They concluded that the combined influence of production well and capillary imbibition reduce the risk of aquifer contamination by ten-fold. Pfunt et al. [11] applied a two-dimensional model to simulate the long-term (300 years) upward migration of FF towards an aquifer in the North German Basin. They deduced that the FF was incapable of reaching the aquifer regardless of the presence of permeable pathways.

The general intention of this study is to assess HF fluid flow through a naturally present fault zone (Fig. 1) during and after the stimulation operation in a HCBF. We constructed a generic, finite element method (FEM) based numerical model to simulate short-term HF fluid migration into overburden layers with the presence of a fault zone extending from a HCBF to a shallow aquifer. The simulation replicates two HF stages, i.e. the fracturing-procedure and the shut-in time intervals. This study attempts to extend upon reviewed literature by examining the degree of influence of each parameter (e.g., operational parameters, such as, injection pressure, or pathway and overburden properties) by systematic parameter variation. Selecting suitable boundary conditions is an important part of simulating fluid transport towards overlying layers, and potentially carries a noticeable influence on the results. An important aspect of our modeling approach is to investigate the effect of domain boundary conditions on migration of FF into shallow aquifers.

2. Conceptual Model

The initial step of developing a generic numeric model representative of sedimentary basins included carrying out a comprehensive literature review. Majority of data integrated was collected from available modelling studies [2,8–10,12]. The general intent of this study is to build a conceptual model which could be applicable for further investigation of contamination leakage due to HF stimulation in HCBF, not to investigate a specific formation. To assess the potential worst-case scenario, a relatively simple model with a permeable continuous fault zone connecting the HCBF to the overlying aquifer was considered. The fundamental reason for implementing a basic model is to improve the understanding of the FF transport mechanisms occurring within geologic layers. However, the purpose of this study is not to describe HF developing processes relating to fracture propagation, dilatation, and network formation creation; but rather applies assumptions of an already formed, fully-matured fracture network being present

prior to injection. Therefore, this model utilizes the assumption that hydro-fractured networks extend to the top of the HCBF. This investigation concentrates on the migration of FF into an above-lying aquifer within short time scales, therefore, the model simulates a time frame representing typical injection and shut-in periods of HF operations.

A two-dimensional, vertical cross-section geological conceptual model, comprised of three hydrostratigraphic units including: (1) aquifer, (2) overburden, and (3) HCBF, is considered. Additionally, a single, naturally occurring fault zone extending from the HCBF to the overlying groundwater source was implemented. The consideration of a continuous fault zone is a conservative assumption similar to those employed in previous studies (e.g., Kissinger et al. [2], Mayer [8] Gassiat et al. [10]). However, the presence of a connecting fault zone may not necessarily apply in nature that frequently, therefore, we also considered cases with a fault zone not reaching the aquifer [13]. Two failure scenarios are considered to investigate HF fluid transport through a connected fault zone including: (1) FS1; the presence of a HCBF; (2) FS2; the absence of a HCBF (Fig. 1). With respect to the symmetry, the left edge of the model was assigned with a no-flow boundary. The top boundary of the domain was considered as the bottom of the aquifer. Instead of simulating flow in the aquifer explicitly, we defined the aquifer as a constant pressure boundary at the top of the domain set to 1 MPa as aquifer pressure. We assumed that any possible contamination (FF) that reaches the top boundary of the model enters the overlying aquifer. Different boundary conditions results in different types and degrees of impact on upward migration of FF across the overburden. To further understand the effect of different boundary conditions on contaminant transport, each scenario was divided into four sub-scenarios varying boundary conditions: (1) open (right: constant-head pressure boundary, bottom: pressure boundary); (2) closed (right: no-flow boundary, bottom: no-flow boundary); (3) semi l (right: constant-head pressure boundary, bottom: no-flow boundary); (4) semi ll (right: no-flow boundary, bottom: pressure boundary) (Fig. 1).
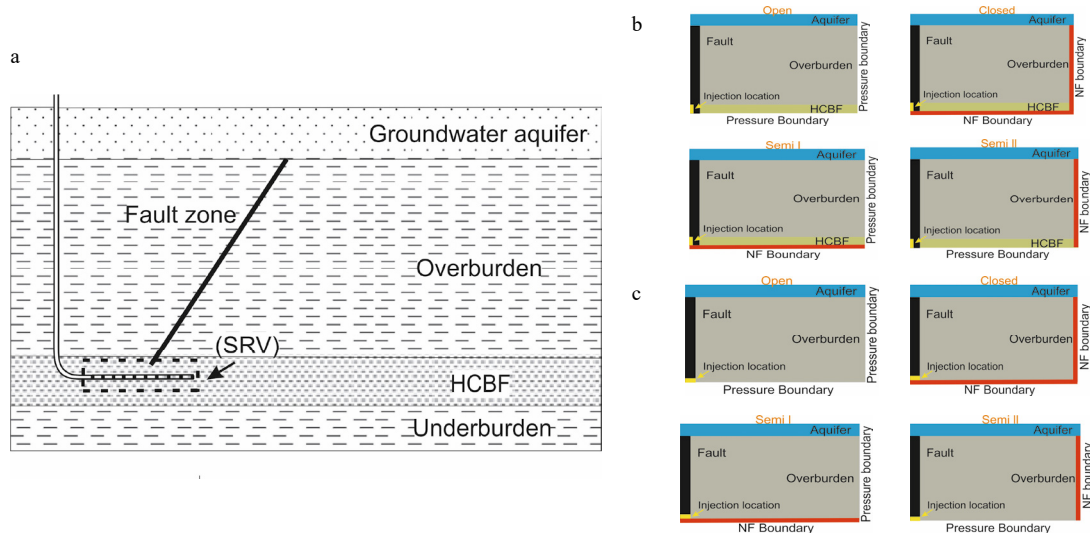

Fig. 1. A cross section schematic of a fault zone intersecting the stimulated reservoir volume (SRV) in a hydrocarbon bearing formation and the conceptual representation of the Source (HCBF) – Pathway (Conductive Fault)– Receptor (Groundwater aquifer) concept. (b) FS1: with considering the HCBF; (c) FS2: without considering the HCBF.

The model domain was defined by dimensions of 3 km width, with a depth varying from 1.225 km to 2.225 km (Fig. 1). All strata were considered as homogeneous and anisotropic. Anisotropic conditions were assigned because typically horizontal permeability is generally larger than vertical permeability often by several orders of magnitude [14,15]. The conductive fault zone was considered as homogeneous and isotropic with a higher permeability compared to the surrounding overburden and hydrocarbon layers. The width of the fault zone is assumed as 10 m, parallel to the left edge of the model domain. Fault permeability in the overburden layer is larger than its permeability in the hydrocarbon layer by three orders of magnitude. Depth related relationships for temperature, pressure, and salinity

were implemented to calculate reservoir pore fluid properties (density and dynamic viscosity) [16]. An initial salinity of $100 \ kg/m^3$ was set at $200 \ m$ depth, and a moderate salinity gradient of $0.11 \ kg/m^3 \ /m$ was assigned [10,11]. These salinities are adopted to those in the North-German Basin, where maximum salinities can reach up to $250 \ kg/m^3$ close to Zechstein halite deposits. Density differences between the injected FF and brine lead to buoyancy forces. Salinity increasing with depth, increases brine density, thus reducing potential of vertical flux through overlying strata [2]. As high salinities are common in large sedimentary basins [17], we investigated the effect of a wide range of salinities on FF upward migration. An initial temperature at the top of aquifer was assumed at 12 ℃ with average temperature gradient of $0.03 \ ℃/m$ which is the common average geothermal gradient [9].

The hydraulic fracturing operation was simulated by applying a constant head boundary condition for a specified time period directly at the edge of the fault zone. Following the injection time period, the shut-in period was monitored, which is considerable longer compared to the injection duration. The determination of the necessary degree and duration of hydraulic pressure applied to the system primarily depends on the petrophysical properties of the HCBF, the depth, and initial lithological pressure [11]. For the simulation of the wide array of injection pressures observed in the industry, a sensitivity analysis of excess pressure values was performed. During all injection periods, the HF pressures are held constant for the 20-hour duration. The shut-in period following the injection was observed for pressure alterations in the system. Notably, the absence of a pressure reduction occurring between the borehole (maximum) and the fault zone (relatively lower) should be viewed as a very conservative assumption. Considering a constant pressure at the fault zone to simulate a HF operation leads to an overestimation of the FF derived contaminant concentration in the aquifer. For the base case models, simulations of HF and shut-in periods were conducted in two consecutive runs. Total simulation time is 60 hours, of which the HF time is 20 hours (initial run), and the remaining 40 hours represents the shut-in period and pressure decay period (second run). The output from the fracturing injection simulation was assigned as initial conditions for the second run. Since the purpose of this study is primarily to assess parameter influence on upward migration of FF, the sensitivity analysis was conducted only for the injection time period (initial run). Therefore, by obtaining a "base case" reference model output from predefined mid-range values, individual parameter sweeps were conducted to identify the degree of numerical output alterations. The base case value of each parameter of interest and its range of variation of the variables in the sensitivity analysis are presented in Table 1. The value of parameters used for all the simulations are shown in Table 2.

Table 1. Parameters used for base case models and sensitivity analysis.

Parameters	Value	Variation	References
Overburden thickness, m	1300	$1100 - 2100$	[18,19]
Fault width, m	10	$5 - 20$	[10]
Overburden permeability, m^2	1×10^{-16}	$1 \times 10^{-18} - 1 \times 10^{-15}$	[10]
Overburden anisotropy ratio	100	$1 - 1000$	[14,15]
Fault permeability, m^2	5×10^{-11}	$2 \times 10^{-11} - 1 \times 10^{-10}$	[10,12]
Fault porosity	0.1	$0.08 - 0.12$	[8]
Salinity, kg/m^3	Depth dependent	$150 - 350$	[17]
HF injection pressure, MPa	30	$20 - 45$	[2,11]

Table 2. Parameters used in all of the simulations.

Parameters	Value	References
Domain length, m	3000	[20]
Aquifer thickness, m	100	[10]
Reservoir permeability, m^2	1×10^{-19}	[10]
Aquifer pressure, MPa	1	[9]
Overburden porosity	0.03	[10]
Reservoir porosity	0.03	[10]
Reservoir thickness, m	25	[10]
Aquifer temperature, ℃	12	[9]
Reservoir overpressure gradient, KPa/m	13	[10]
Initial salinity at 200 m, kg/m^3	100	[10]
Fault anisotropy	1	[10]
Geothermal gradient, $℃/m$	0.03	[9]
Reservoir anisotropy	1000	[14,15]
Molecular diffusivity of solutes in pure fluid, m^2/s	1×10^{-9}	[10]
Fracturing fluid density, kg/m^3	1000	[10]

3. Mathematical and numerical model

Fracking fluid (FF) is a water-based fluid with fine sand grains and critical additives being primarily water soluble. Flow and transport via gas migration is considered unlikely because after a certain transport distance gas and liquid phases are separate and continue individually [21]. Therefore, the model assumes single phase (water) flow comprising two-components. The model assumes the fluid dissolved substances as a conservative tracer, i.e. concentration losses from sorption and degradation processes are ignored. Lastly, the flow and transport model does not account for geomechanical effects, such as dynamic changes in pore volume and permeability due to stress changes. The following set of equations describe the flow and solute transport in a porous media system [22,23]:

$$u = -K \frac{1}{\mu_w}(\nabla p_w + \rho_w \text{g}) \tag{1}$$

$$\frac{\partial \phi \rho_w}{\partial t} - \nabla . \left[K \frac{\rho_w}{\mu_w}(\nabla p_w - \rho_w \text{g}) \right] = 0 \tag{2}$$

$$\frac{\partial c_i}{\partial t} - \nabla \cdot \left(D_{pm}^i \nabla c_i \right) + u \cdot \nabla c_i - R_i = 0 \tag{3}$$

where u is the Darcy velocity or specific discharge vector (SI unit: m/s), K is the intrinsic permeability of the porous medium (SI unit: m^2); μ_w is the dynamic viscosity of water (SI unit: $Pa.s$); p_w is the fluid's pressure (SI unit: Pa), ρ_w is the density (SI unit: kg/m^3); g is the vector of gravitational acceleration; c_i is the concentration of the chemical species i (SI unit: mol/m^3); D_{pm}^i is the diffusion coefficient of component i (SI unit: m^2/s); R_i is the reaction rate, which is considered zero in our case (this is a conservative assumption that the FF is not being absorbed by the porous media, nor interacts with it).

The mathematical model is implemented in COMSOL 5.2.a Multiphysics simulator, using the pre-existing Subsurface Flow Module by coupling the Darcy's Law interface with the Transport of Diluted Species in Porous Media interface. COMSOL Multiphysics is a finite element analysis (FEA) software package for various physics and engineering applications which discretizes the mathematical model by the finite element method.

4. Results and discussion

The modeling results of the two main failure scenarios (FS1, FS2), respectively the corresponding eight sub-scenarios (defined in chapter 2) are described and compared to better understand boundary influences on the upward movement of FF into overlying layers. The results are provided as FF concentration breakthrough curves, concentration profiles along the fault zone, pressure profiles along the fault zone, and depth of 2% concentration threshold.

To simulate the defined scenarios, a very fine, unstructured, free-triangular, finite element mesh was generated. A sensitivity analysis with regard to the mesh size was conducted, identifying the optimum element size in which alterations to it produce minimal influences on the results. The applied mesh consisting of 105,368 elements is shown in Fig. 2.a. An example of the spatial distribution of the FF concentration over the domain is illustrated in Fig. 2.b. For this particular case (FS2; sub-scenario: open), FF migrated up the fault, and the 2% concentration threshold reached a depth of 330 m (respectively 970 m up the fault from the source location) following the shut-in period. This modeling scenario demonstrates that the FF transported up the fault system did not significantly contaminate the shallow aquifer.

Figure 3 compares FF concentration breakthrough curves for the base cases of all eight sub-scenarios (FS1 and FS2). It was observed that the vertical extent of the FF concentration increased throughout the injection period, and maintained the level during the shut-in period. In addition, FF plume spread more laterally during the shut-in period. The sub-scenarios "open" and "semi I" had lower concentrations arriving at the aquifer boundary when compared to sub-scenarios "closed" and "semi II". This applies to both main failure scenarios (i.e. FS1, FS2). This behaviour can be explained by the pressure distributions along the fault zones. The no-flow boundary conditions do not allow the fluid to leave the domain and implicitly lead to a higher increase of fluid pressure in the entire domain compared to the Dirichlet pressure boundary condition, which allows fluxes outside of the domain. Therefore, as illustrated by Fig.

4.i and Fig. 5.i, the pressure gradients along the fault for sub-scenarios "closed" and "semi II" are higher than "open" and "semi I", leading to higher fluxes, and implicitly larger FF concentrations.
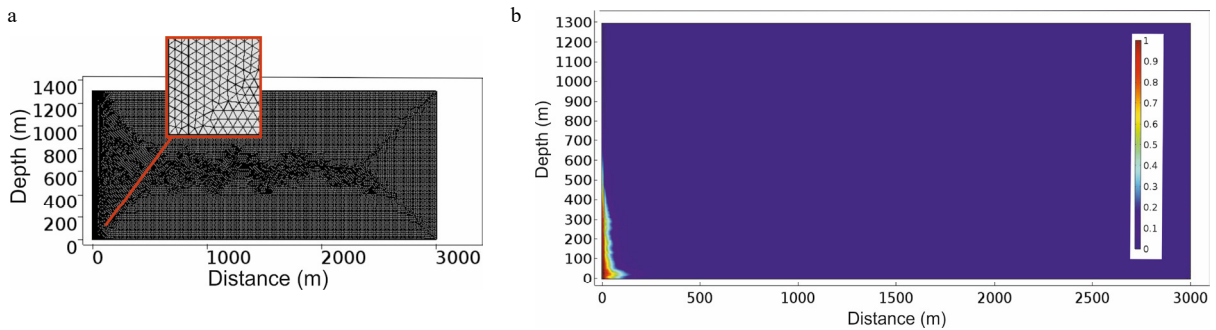

Fig. 2. (a) Finite-element mesh implemented for the numerical simulation; (b) Fracking fluid concentration at the end of shut-in period (FS1; sub-scenario: open).

Comparing the two failure scenarios, it was observed that for FS1 the fluid migrated further up fault (shown by comparing both sets of four sub-scenarios). This is attributed to the overpressure within the HCBF. Maximum concentration was monitored in the receptor (1.2% of total injected concentration) in FS1, the "semi II" sub-scenario. In this scenario, 2% level of concentration was reached to the height of 1236 m. The lowest FF concentration in the aquifer was observed in FS2; sub-scenario "open". In this case, 0.16% of the initial concentration entered the aquifer and the height of 2% concentration threshold reached 970 m.

When observing strictly the base case scenario for FS1 in sub-scenarios "closed" and "semi II", changing the bottom boundary from the chosen constant-pressure magnitude to no-flow led to an increase of lateral spreading of FF in the overburden, thus decreasing the aquifer concentration distribution. Moreover, when observing the base case scenario for FS2, both sub-scenarios "closed" and "semi II" led to the similar aquifer contamination concentrations. Therefore, for this failure scenario, it is concluded that while the right side of the domain maintained constant-head pressure boundary, a change in the bottom boundary from the chosen constant pressure magnitude to no-flow has negligible effect on the vertical extent of FF migration and the respective concentration distribution at the aquifer base. From all of the investigated sub-scenarios, it was observed that changing the right domain boundary has a greater influence on the FF concentration into the aquifer in comparison to changing the bottom boundary condition.
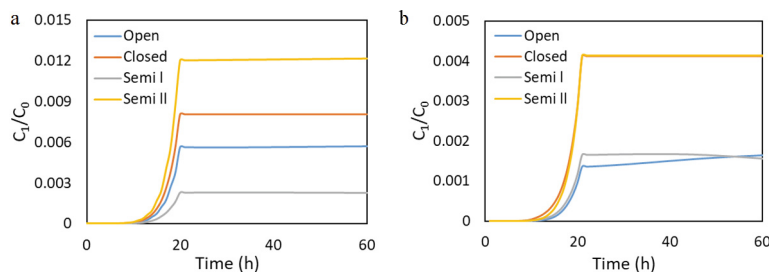

Fig. 3. Fracking fluid concentration breakthrough curves throughout HF and shut-in period, observed at the aquifer base (a) FS1; (b) FS2.

4.1. Sensitivity analysis

We performed a sensitivity analysis to understand the influence of key operational parameters and reservoir physical properties. The key parameters, and their range variations, were selected based on the aforementioned modelling studies (Table 1). The parameters investigated were fault permeability (K_f), effective fault porosity ($\emptyset_f$), fault width (W_f), overburden thickness (h_O), overburden permeability (K_O), overburden anisotropy ratio (A_O), HF injection pressure (P_{inj}), and salinity (S). We also considered cases with the fault zone does not extending to the aquifer, as well as instances where varying fault zone inclination are present [24]. The FF concentration at the aquifer

base at the end of the injection period is shown in Fig. 4, and 5 (a-h). These figures demonstrate the sensitivity analysis results for the investigated key parameters in the eight sub-scenarios (FS1 and FS2). The pressure distribution along the fault zone for base cases are also presented in Fig. 4.i, and 5.i. The model results showed FF concentration does not reach the aquifer when the inclination of the fault is less than 90 degrees. In addition, scenarios observed without a continuous permeable pathway connecting the HCBF to the overlying aquifer resulted in a limited vertical migration of fluids. In this case, the vertical transport of contaminants is strongly related to the vertical extend of the fault.

The obtained results showed that a relatively small increase in the fault permeability led to a higher FF contamination distribution in the aquifer. FF did not reach the aquifer base when the permeability of the fault was less than $4 \times 10^{-11} \ m^2$, however, the highest aquifer contamination occurred when the fault permeability was higher than $7 \times 10^{-11} \ m^2$. For all sub-scenarios, a HF injection pressure higher than 30 MPa resulted in the aquifer contamination. An excess in the HF pressure led to a quicker upward migration of FF into the fault zone and the surrounding matrix. Also, an increase in the fault width showed a higher vertical transport of FF towards the aquifer. The contamination distribution in the aquifer was decreased with an increase of overburden thickness, and it was negligible for cases where the HCBF was deeper than 1700 m. The increase of overburden permeability, and overburden anisotropy resulted in a spreading migration of FF in the overburden, and therefore, less contaminant arrival into the aquifer. Furthermore, salinity gradients have the potential to exclusively influence the transport of FF into overburden layers. The FF propagation height was reduced with an increase of the implemented salinity in the domain.
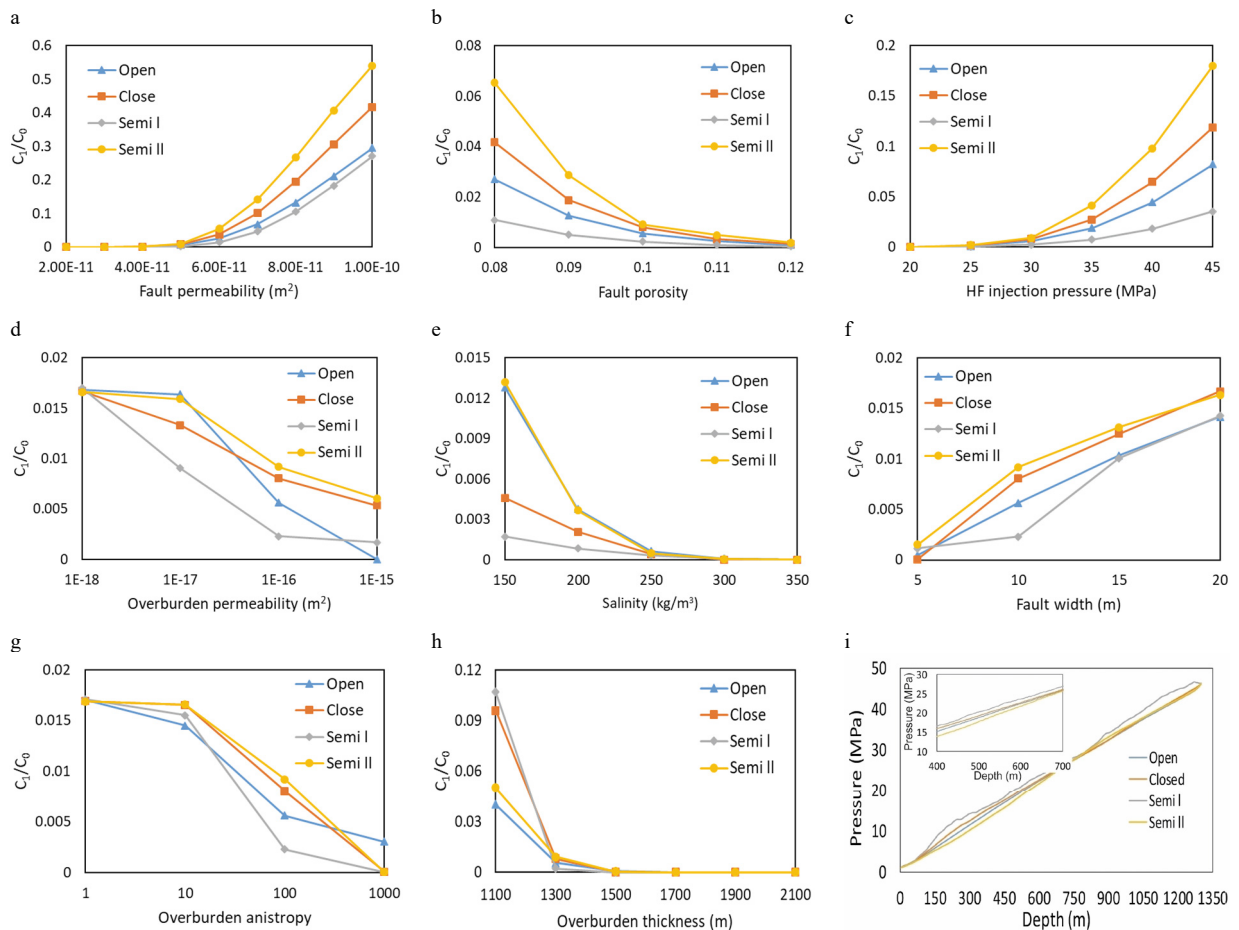

Fig. 4. FS1 (model considering the presence of HCBF): (a-h) fracking fluid concentration in the aquifer at the end of the injection period for each investigated parameter range; (i) pressure profile along the fault zone for four "base-case" sub-scenarios.
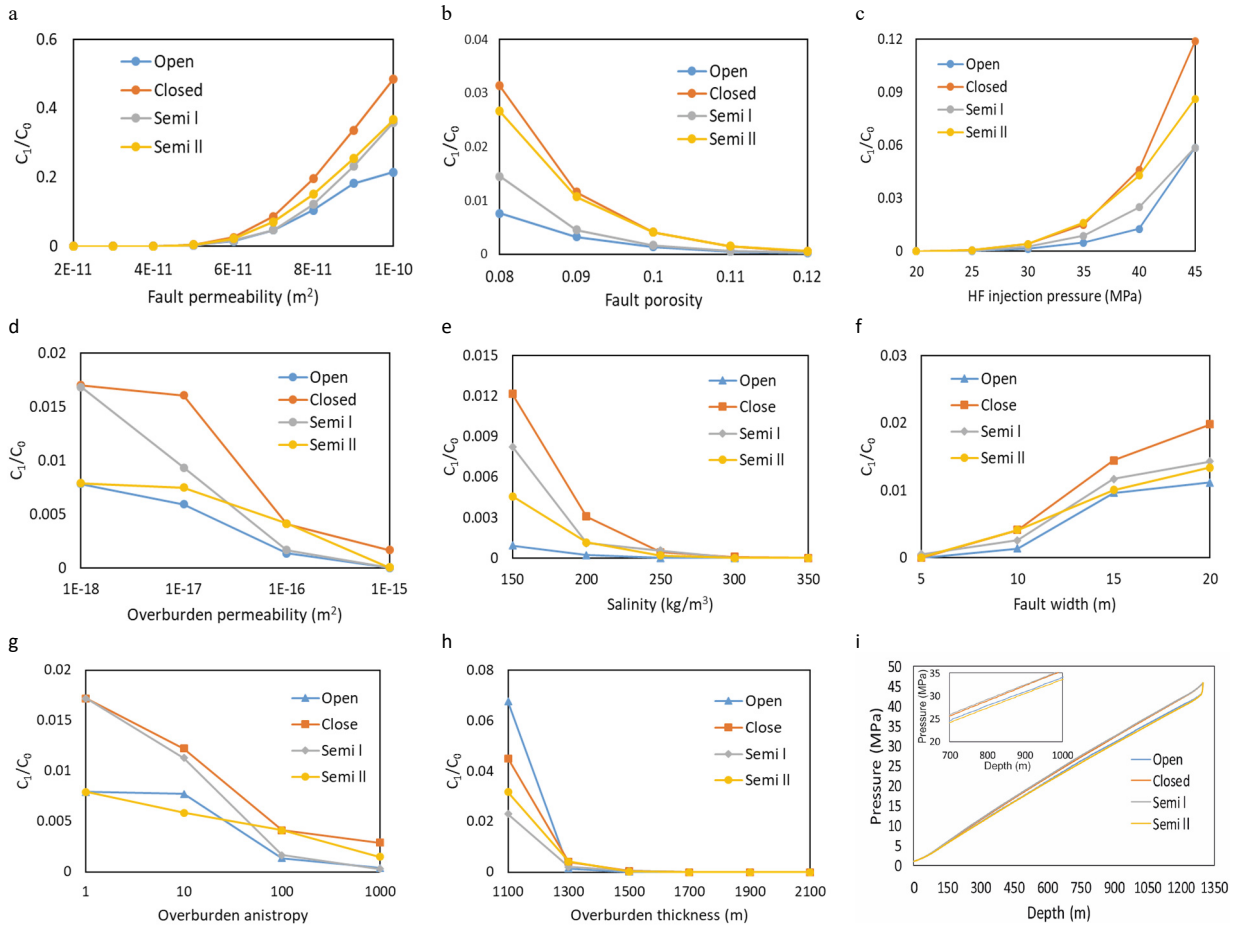
Fig. 5. FS2 (model not including the presence of HCBF): (a-h) fracking fluid concentration in the aquifer at the end of the injection period for each investigated parameter range; (i) pressure profile along the fault zone for four "base-case" sub-scenarios.

The results presented in Fig. 4, and 5 demonstrate the influence of each key parameter on the upward transport of FF towards the receptor. To rank the importance of studied parameters (defined in Table 1) for each modelling sub-scenario, the difference between the resulting concentrations at the aquifer base corresponding to the minimum and maximum parameter range values was calculated using equation 4. The parameter importance for all studied sub-scenarios is assessed by computing the mean value. The mean value ($ME_{\Delta I}$) is calculated using the ΔI value (obtained applying equation 4) from all eight sub-scenarios using equation 5. $ME_{\Delta I}$ represents the influence of each key parameter on the transport distance of the FF to overlying layers, independent of the scenario and domain boundary conditions.

$$\Delta I = (C_1/C_0)_{max} - (C_1/C_0)_{min} \tag{4}$$

$$ME_{\Delta I} = \frac{\sum_{n=1}^{n=8} \Delta I_n}{8} \tag{5}$$

where C_1/C_0 represents the contamination concentration at the aquifer base, and *n* stands for the number of sub-scenarios. Fig. 6.a describes the relative impact of each parameter (by applying equation 4) for all eight sub-scenarios. The influence of every parameter for each individual scenario, and the different types of boundary conditions is evident. Fig. 6.b illustrates the influence of each parameter (by applying equation 5). The caclulated values, ΔI and $ME_{\Delta I}$, represents the degree of influence each parameter imposes on the output result. A positive value represents an increase in concentration at the aquifer base, while a negative value represents decrease. Fault permeability is the most

influential parameter, as its increase led to a significantly higher concentration distribution at the aquifer, including its vertical migration. HF injection pressure was the second most influential parameter, with a distinct correlation with the vertical extent of fluid migration. Overburden thickness, the third most important factor, has an inverse effect on concentration distribution. Therefore, the potential contamination threat to a shallow aquifer obviously declines with an increase in hydraocarbon reservoir depth. Based on the simulation results, short-term contamination risks from HF in deep hydrocarbon reservoir can be considered minimal. Furthermore, an increase in overburden permeability and overburden anistropy ratio causes a decrease in concentration at the aquifer base due to the increased importance of lateral spreading of fluids into overburden layers. According to Fig. 6, physical properties of the fault zone are the most influential parameters dictating the upward transport of FF into the aquifer. The modelling results demonstrate the inverse effect of salinity on the concentration distribution at the aquifer. This strengthens the argument that high salinities in sedimentary basins decrease the potential for upward migration of brine and FF into shallow aquifers.
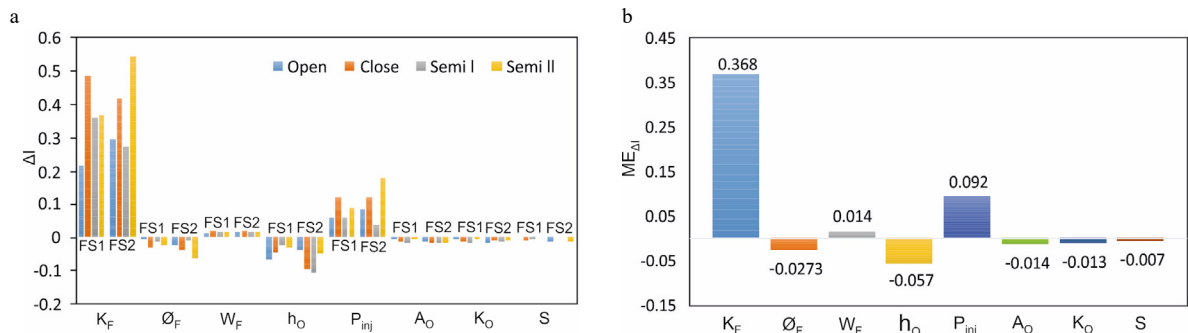

Fig. 6. The ranked impacts of key investigated parameters on upward migration of FF along a fault towards the aquifer: (a) (a) parameter importance of the individual sub-scenarios (eq. 4); (b) the calculated mean value of parameter importance of all sub-scenarios (eq. 5) for the each investigated parameter .

5. Conclusions

In this paper, two main scenarios were selected based on an FEP approach to investigate FF transport along a fault zone into shallow aquifers during and after HF operation. To assess the effects of boundary conditions on the modelling results, each scenario is divided into four sub-scenarios, including: (1) open; (2) closed; (3) semi l; (4) semi ll. A sensitivity analysis was performed to study the relative influence of reservoir properties and operational parameters on upward transport of FF into shallow aquifers. The numerical simulation results showed fault properties, and particularly fault permeability, are the most influential parameters inducing migration of contaminants from a HCBF along a fault zone. HF injection pressure, reservoir depth, and overburden properties also play important roles in the upward flux of contaminants. The modelling results demonstrate that without the presence of a continuous vertical fault zone, FF does not reach the aquifer. Furthermore, The probability of contamination of shallow aquifers by upward migration of FF through the fault zone is insignificant during and after the HF period. However, the FF concentration in the aquifer may increase for certain hydraulic conditions (e.g., high fault permeability, and porosity), indicating that the proper assignment of boundary conditions is essential. Eventhough, HF operations are designed so that the SRV and its adjacent hydraulically influenced areas do not intersect conductive faults, such possibility cannot be neglected. This possibility may occur either as a result of undetected geological features (e.g., insufficient resolution of the geo-physical charactierzation, dormant faults which are reactivated during stimulation), or as human error in the designing or conduction of HF operations. This study is generic, demonstrating that quantitative risk assessment can be performed on the basis of Source-Pathway-Receptor and FEP approaches by means of forward modelling. Nevertheless, for a particular field study, reliable data acquisition must be conducted.

Acknowledgements

References

[1] Pruess K, Narasimhan T. A practical method for modeling fluid and heat flow in fractured porous media 1982.

[2] Kissinger A, Helmig R, Ebigbo A, Class H, Lange T, Sauter M, et al. Hydraulic fracturing in unconventional gas reservoirs: Risks in the geological system, part 2: Modelling the transport of fracturing fluids, brine and methane. Environmental Earth Sciences 2013;70:3855–73. doi:10.1007/s12665-013-2578-6.

[3] Lange T, Sauter M, Heitfeld M, Schetelig K, Brosig K, Jahnke W, et al. Hydraulic fracturing in unconventional gas reservoirs: risks in the geological system part 1. Environmental Earth Sciences 2013;70:3839–53. doi:10.1007/s12665-013-2803-3.

[4] Tatomir A, McDermott C, Edlmann K, Bensabat J, Wiener H, Goren Y. D3.1 Update of FEP database (Version 2). 2015.

[5] Wiener H, Goren Y, Bensabat J, Tatomir A, Edlmann, Katriona McDermott C. D4.1 Ranked FEP list. 2015.

[6] Gläser D, Dell A, Tatomir A. An approach towards an FEP-based model for risk assessment for hydraulic fracturing operations. Energy Procedia 2016;97:Pages 387-394.

[7] Tatomir A, Sauter M, Foghi M, Taherdangkoo R, Sauter M, Bensabat J, et al. D3.2 Characterization of the Key FEP risk scenarios. 2016.

[8] Myers T. Potential Contaminant Pathways from Hydraulically Fractured Shale to Aquifers. Ground Water 2012;50:872–82. doi:10.1111/j.1745-6584.2012.00933.x.

[9] Reagan MT, Moridis GJ, Keen ND, Johnson JN. Numerical simulation of the environmental impact of hydraulic fracturing of tight/shale gas reservoirs on near-surface groundwater: Background, base cases, shallow reservoirs, short-term gas, and water transport 2015:1–31.

[10] Gassiat C, Gleeson T, Lefebvre R, McKenzie J. Hydraulic fracturing in faulted sedimentary basins: Numerical simulation of potential contamination of shallow aquifers over long time scales. Water Resources Research 2013;49:8310–27. doi:10.1002/2013WR014287.

[11] Pfunt H, Houben G, Himmelsbach T. Numerical modeling of fracking fluid migration through fault zones and fractures in the North German Basin. Hydrogeology Journal 2016. doi:10.1007/s10040-016-1418-7.

[12] Birdsell DT, Rajaram H, Dempsey D, Viswanathan HS. Hydraulic fracturing fluidmigration in the subsurface: A review and expanded modeling results. Water Resources Research 2015;51:7159–88. doi:10.1002/2015WR017810.

[13] Edlmann K, McDermott C. D2.3 Hydro-geo-chemo-mechanical facies analysis relative to gas shales's of key basins 2016.

[14] Freeze R, Cherry J. Groundwater, 604 pp 1979.

[15] Neuzil C. How permeable are clays and shales? Water Resources Research 1994.

[16] Batzle M, Wang Z. Seismic properties of pore fluids. Geophysics 1992.

[17] King G. Hydraulic fracturing 101: what every representative, environmentalist, regulator, reporter, investor, university researcher, neighbor and engineer should know about. SPE Hydraulic Fracturing Technology Conference 2012.

[18] Administration USEI. World shale gas resources: an initial assessment of 14 regions outside the United States. 2011.

[19] EIA U. Review of emerging resources: US Shale gas and shale oil plays. Energy Information Administration, US Department of 2011.

[20] Brownlow JW, Yelderman JC, James SC. Spatial Risk Analysis of Hydraulic Fracturing near Abandoned and Converted Oil and Gas Wells. Groundwater 2016. doi:10.1111/gwat.12471.

[21] Schwartz M. Modelling the performance of liquefied petroleum gas fracking versus water fracking. International Journal of Petroleum 2016.

[22] Helmig R. Multiphase flow and transport processes in the subsurface: a contribution to the modeling of hydrosystems. 1997.

[23] Bear J. Dynamics of fluids in porous media. 2013.